Single-Quantum-Wire Waveguide Modulator with High on/off Ratio and Low Voltage Swing

S. Palmgren,[1,2] H. Weman,[1,2] A. Rudra,[1] and E. Kapon,[1]
[1]Laboratory of Physics of Nanostructures, Institute of Quantum Electronics and Photonics, Swiss Federal Institute of Technology (EPFL), CH-1015 Lausanne, Switzerland.
[2]Department of Physics, Linköping University, S-581 83 Linköping, Sweden.
susanna.palmgren@epfl.ch

We demonstrate a waveguide modulator with an on/off ratio 50:1 at a 5 V voltage swing using a single quantum wire in a sub-micron sized waveguide. The modal absorption of the single wire is 140 cm^{-1}.

Keywords: quantum-wire, electro-absorption modulator, waveguide, semiconductor modulator

Introduction

Semiconductor quantum well (QW) waveguide intensity modulators have attracted considerable interest due to their high performance and capability of monolithic integration with laser diodes [1]. Important parameters for applications of such electro-absorption modulators are high on/off ratio, low driving voltage, high speed, low chirp and compact size. These modulators are based on either the quantum-confined Stark effect (QCSE) or quenching of exciton absorption due to phase-space-filling (PAQ). Due to the enhancement of the exciton oscillator strength in one dimensional structures, these effects are expected to be strongly modified as compared to QWs [2-3]. Here, we report on an efficient electro-absorption modulator based on a single quantum wire (QWR) embedded in a sub-micron sized V-shaped dielectric waveguide. We obtain a high on/off ratio (50:1) with a low voltage swing (5V) at 820 nm by using a 500 µm long QWR waveguide.

Experimental

The QWR waveguide samples were grown by low-pressure organometallic chemical vapor deposition (OMCVD) on n^+-doped (100) GaAs substrates patterned with 250 µm spaced V-grooves along the [1-10] direction. Each V-groove contains a dielectric AlGaAs/GaAs waveguide that incorporates a single self-organized GaAs QWR placed in the core region of a V-shaped AlGaAs optical waveguide [4]. The core region has a total thickness of 295 nm and is clad with 1 µm thick *n*- and *p*-doped $Al_{0.65}Ga_{0.35}As$ layers on the bottom and top of the core layer, respectively. The QWR was displaced upwards from the center of the core region in order to obtain an optimal mode confinement factor , which was estimated to be 0.1 % for the single QWR [4]. The $Al_{0.30}Ga_{0.70}As$ waveguide core was *n*-doped to a distance of 25 nm from the QWR in order to have electron filling in the wire at flatband (FB). The V-shape of the dielectric waveguide yields a sub-µm sized, heart-shaped optical mode that is well confined in the core region of the waveguide according to our calculation of the electromagnetic field distribution of the optical modes [4]. A transmission electron microscopy (TEM) micrograph of a V-shaped optical waveguide region containing a single crescent-shaped QWR is shown in Fig. 1.

For the top ohmic *p*-contacts, a 100 µm wide Ti/Au stripe was centered on top of the V-groove, and the ohmic *n*-contact was obtained by evaporating Ni/Ge/Au on the backside followed by annealing at 420°C. The waveguide samples were then cleaved and contacted by bonding wires. The *I*-*V* characteristics typically showed a forward turn-on voltage of about 1.3 V with a dark current of less than 5 µA at 5 V reverse bias.

Waveguide transmission spectra were measured at room temperature (RT) as a function of the applied voltage that was varied from 1V to –5 V. For optical excitation we used a Ti-Sapphire laser

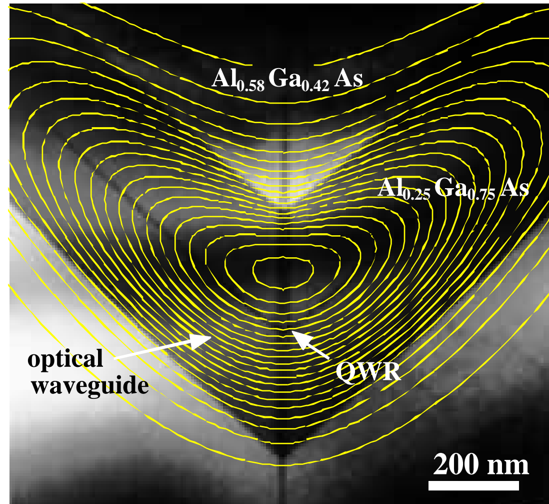

Fig.1. TEM picture of a typical V-shaped GaAs/AlGaAs dielectric waveguide with a single GaAs quantum wire. Contour lines show the mode intensity distribution of the monomode structure.

with the incoming light linearly polarized along the [110] (TE polarization) or [001] (TM polarization) directions. The mechanically chopped light was coupled into the single V-groove QWR waveguide with a microscope objective at the sample edge and guided along the QWR axis ([1-10] direction). This corresponds to the excitation of mainly the fundamental waveguide eigenmode. The out-coupled light was collected by a second microscope objective and detected with a silicon photodiode using a lock-in amplifier. To verify that the coupled light spot was centered properly on the V-shaped waveguide core, the front- and back-side facets of the device were monitored in near-field using Si CCD cameras. Absorption spectra, ( ), are derived from the measured transmission spectra, T( ), by the relationship:

$$(\ ) \quad - \ln[T(\ )] \qquad (1)$$

Results and Discussions

Figure 2 (a) shows the RT absorption spectrum of a 500 μm long QWR waveguide device for TE polarization with a bias of 1 V applied (near flatband). A very sharp absorption edge is observed near 820 nm with several broad peaks seen in the absorbing part of the spectrum. The spectrum was measured by using a relatively low waveguide-coupled power, estimated to be near 1 μW, which was found to be well below the threshold power that causes absorption bleaching. The exact power coupled into the waveguide structure is however difficult to determine exactly, since the coupling losses depend critically on the angle and focus of the laser spot as well as on the amount of reflection loss.

For the waveguide sample discussed above, the QWR heterostructure was intentionally *n*-type doped so that about 4 electron subbands should be filled in the QWR at flatband. From previous photoluminescence (PL) and PL excitation (PLE) measurements on an *undoped* GaAs/$Al_{0.30}Ga_{0.70}As$ V-groove QWR of similar size, the estimated ground-state transition is expected to be near 1.46 eV (850 nm) at RT with a 1D lateral subband spacing of around 25 meV.

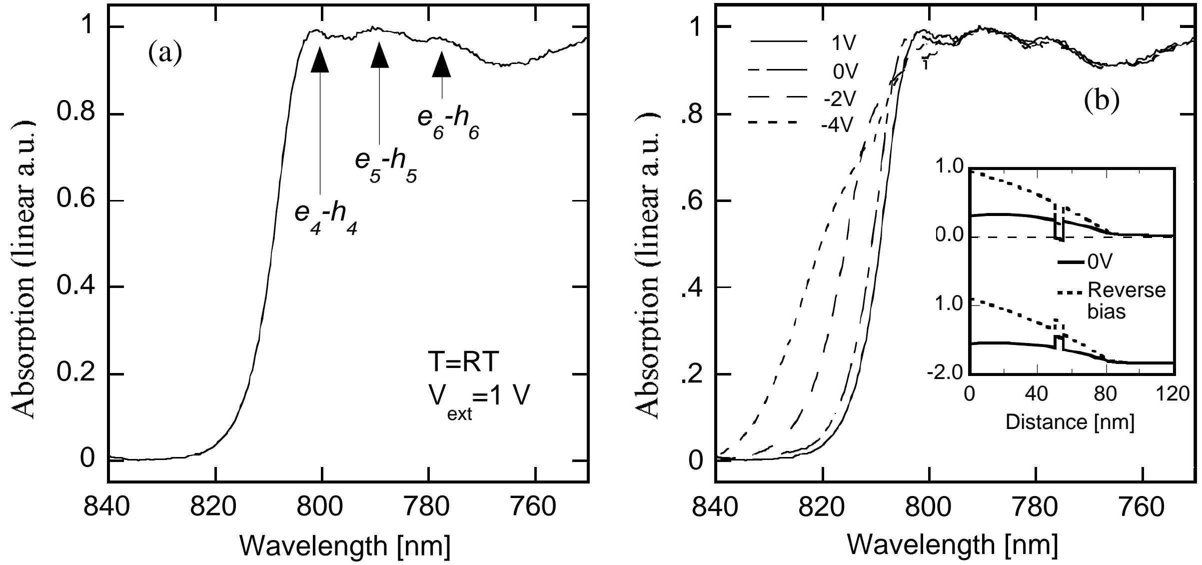

Fig. 2. (a) Linear absorption spectrum at RT of a 500 µm long QWR waveguide device for TE polarization with a bias of 1 V applied (near flatband). The modal absorption coefficient due to the single QWR at the band edge is estimated to be140 cm^{-1}. (b) Electro-absorption spectra at RT of the 500 µm long QWR waveguide device for TE polarization as a function of the applied reverse bias voltage. The inset shows the calculated band-diagram at 0V and under reverse-bias.

The sharp absorption edge near 820 nm (1.51 eV) observed in Fig. 2 (a) is therefore interpreted to be due to the transition of an electron from the valence band to the Fermi-level in the QWR somewhere between electron levels number four and five. Lower transitions are effectively absent due to the phase-space absorption quenching (PAQ) effect [5]. The three broad peaks observed in Fig. 2 (a) are interpreted as due to transitions to electron levels n = 4, 5 and 6. The measured absorption coefficient due to the single QWR at the band edge is 140 cm^{-1}. With an estimated optical confinement factor, = 0.1, this yields a QWR material absorption coefficient as high as 14 000 cm^{-1}.

Fig. 2 (b) shows the electro-absorption spectra of the 500 µm long QWR waveguide device for TE polarization as a function of the applied reverse bias voltage. A clear redshift of the absorption edge is seen as the reverse bias is increased. Initially, this redshift is quite uniform over the whole absorption edge, but at higher reverse bias the absorption edge becomes less steep due to a stronger redshift at the low energy tail of the absorption edge. If measured at the absorption edge mid-point intensity the redshift is about 11 nm by increasing the reverse bias from 1V to –4V. This redshift can be interpreted as due to a decrease in the electron density in the QWR as the Fermi level is moved lower in the conduction band, as shown in the inset of Fig. 2 (b). This allows the absorption to take place at lower and lower energies (reducing the PAQ effect) as the electron density in the QWR is lowered due to the applied reverse bias. However, due to the setting of an electric field across the QWR potential under reverse bias there is also an additional QCSE effect contributing to the redshift [6]. We believe that the QCSE effect is causing the stronger absorption redshift at the low energy tail of the absorption edge.

Maximum contrast is achieved near 820 nm resulting in an on/off ratio of 50:1 (17 dB) with a voltage swing of 5V (from 1V to –4V). For the present modulator this optimum wavelength is slightly above the absorption edge. While this contrast ratio should be sufficient for device applications and in fact occurs at a lower voltage swing than is achieved with well optimized quantum well modulators [7,8], device is only a first demonstration of a QWR modulator. At present we are investigating modulators with lower filling factors and undoped QWR modulators in order to investigate the PAQ and QCSE effects separately, which will allow to further optimize the modulator performance.

Conclusions

We have measured the electro-absorption modulation in an *n*-type doped single GaAs/AlGaAs QWR, sub-micron sized waveguide modulator at room temperature. We have obtained an on/off ratio of 50:1 with a voltage swing as low as 5V. The observed absorption edge modulation is a combined effect of electron transfer out of the QWR and the quantum confined Stark effect. The measured modal absorption and estimated QWR material gain coefficient due to the single QWR is 140 cm^{-1} and 14 000 cm^{-1}, respectively.

These results make our device attractive both as a discrete, small size low-voltage intensity modulator as well as for future planar integration with V-groove QWR lasers [9].

Acknowledgements

The authors gratefully acknowledge E. Martinet, L. Sirigu, and K. F. Karlsson for assistance in the course of this work. This work was partly funded by the Swedish Foundation for Strategic Research under the “NANOPTO” Consortium.

References

[1] Semiconductor optical modulators, by K. Wakita (Kluwer academic publishers, Boston, 1998).
[2] H. Sakaki, K. Kato, and H. Yoshimura, Appl. Phys. Lett. **57**, 2800 (1990).
[3] H. Ando, H. Oohashi, and H. Kanbe, J. Appl. Phys. **70**, 7024 (1991).
[4] D. Crisinel, M.-A. Dupertuis, and E. Kapon, Optical and Quantum Electronics **31**, 797 (1999).
[5] H. Weman, E. Martinet, M.-A. Dupertuis, A. Rudra, and E. Kapon, phys. stat. sol. (a) **178**, 249 (2000).
[6] H. Weman, E. Martinet, M.-A. Dupertuis, A. Rudra, and E. Kapon, Appl. Phys. Lett. **74**, 2334, (1999).
[7] P.N. Freeman, P. Bhattacharya, M. Jaffe, J. Singh, and X. Zhang, *IEEE J.Quantum Electron.* **QE-32**, 1161, 1996.
[8] O. Blum, J.E. Zucker, T.Y. Chang, N.J. Sauer, M. Divino, K.L. Jones, and T.K. Gustafson, *IEEE Photon. Technol. Lett.* **3**, 327, 1991.
[9] E. Kapon, Optoelectronics- Devices and Technologies, **8**, 429 (1993).